

# Methane Combustion over Pd/ZrO<sub>2</sub>/SiC, Pd/CeO<sub>2</sub>/SiC, Pd/Zr<sub>0.5</sub>Ce<sub>0.5</sub>O<sub>2</sub>/SiC Catalysts

Xiaoning Guo<sup>a,c</sup>, Guojuan Zhi<sup>a,c</sup>, Xiaoyan Yan<sup>a,c</sup>, Guoqiang Jin<sup>a</sup>,  
Xiangyun Guo<sup>a,\*</sup>, Pascal Brault<sup>b,\*</sup>

<sup>a</sup> State Key Laboratory of Coal Conversion, Institute of Coal Chemistry, Taiyuan 030001, PR China

<sup>b</sup> GREMI UMR6606 CNRS - Université d'Orléans BP6744, 45067 ORLEANS Cedex2, France

<sup>c</sup> Graduate University of the Chinese Academy of Sciences, Beijing 100039, PR China

## Abstract

The performances of different promoters (CeO<sub>2</sub>, ZrO<sub>2</sub> and Ce<sub>0.5</sub>Zr<sub>0.5</sub>O<sub>2</sub> solid solution) modified Pd/SiC catalysts for methane combustion are studied. XRD and XPS results showed that Zr<sup>4+</sup> could be incorporated into the CeO<sub>2</sub> lattice to form Zr<sub>0.5</sub>Ce<sub>0.5</sub>O<sub>2</sub> solid solution. The catalytic activities of Pd/CeO<sub>2</sub>/SiC and Pd/ZrO<sub>2</sub>/SiC are lower than that of Pd/Zr<sub>0.5</sub>Ce<sub>0.5</sub>O<sub>2</sub>/SiC. The Pd/Zr<sub>0.5</sub>Ce<sub>0.5</sub>O<sub>2</sub>/SiC catalyst can ignite the reaction at 240°C and obtain a methane conversion of 100% at 340°C, and keep 100 % methane conversion after 10 reaction cycles. These results indicate that active metallic nanoparticles are well stabilized on the SiC surface while the promoters serve as oxygen reservoir and retain good redox properties.

**Keywords:** High surface area SiC; Pd/SiC catalysts; Zr<sub>0.5</sub>Ce<sub>0.5</sub>O<sub>2</sub> solid solution; methane combustion.

\*Corresponding authors:

Fax: +86-351 4050320; Tel: +86-351 4065282

Email: [xyguo@sxicc.ac.cn](mailto:xyguo@sxicc.ac.cn) (X. Y. Guo)

Fax: +33- 2 38 41 71 54; Tel: +33- 2 38 41 71 25

Email: [Pascal.Brault@univ-orleans.fr](mailto:Pascal.Brault@univ-orleans.fr) (P. Brault)

## 1. Introduction

Supported palladium catalysts have been found to have excellent activity toward the catalytic combustion of methane, which has been found to be more environmentally friendly than traditional flame combustion due to lower emissions of  $\text{NO}_x$ , CO, and unburned hydrocarbons<sup>[1,2]</sup>. Usually, the supports of Pd-based catalysts are thermal insulators, such as  $\text{SiO}_2$  and  $\text{Al}_2\text{O}_3$ . The methane combustion is a strongly exothermic reaction, therefore the reaction heat accumulated on isolated metal nanoparticles makes them easily sintered<sup>[3-5]</sup>. It has been established that SiC can be a potentially excellent catalyst support for various reactions since SiC has admirable chemical stability and high thermal conductivity and stability<sup>[6-8]</sup>. Our previous study showed that Pd/SiC catalyst using etched SiC nanowires as the support can completely convert  $\text{CH}_4$  at about  $390^\circ\text{C}$  and run 10 reaction cycles without any decrease in the catalytic activity<sup>[9]</sup>.

It is well known that  $\text{CeO}_2$  and  $\text{ZrO}_2$  are effective promoters for noble-based combustion catalysts because they can enhance the dispersion and stability of metallic active phases. However  $\text{CeO}_2$  is easily sintered at high reaction temperatures, and  $\text{ZrO}_2$  has the drawbacks of high cost and relatively low surface area<sup>[10-13]</sup>. Therefore, researchers have suggested that formation of a  $\text{Ce}_{0.5}\text{Zr}_{0.5}\text{O}_2$  solid solution by adding  $\text{ZrO}_2$  to  $\text{CeO}_2$  can improve oxygen storage capacity, redox properties, thermal resistance and catalytic activity of catalysts at lower temperatures<sup>[14-17]</sup>. In this work, we investigate Pd/SiC catalysts modified by  $\text{CeO}_2$ ,  $\text{ZrO}_2$  and  $\text{Zr}_{0.5}\text{Ce}_{0.5}\text{O}_2$  solid solution respectively, which show excellent activity and stability for methane combustion.

## 2. Experiments

### 2.1 Catalyst Preparation

The catalysts are 1wt.% Pd supported on either SiC ( $S_{\text{BET}}=50.8\text{m}^2/\text{g}$ )<sup>[18, 19]</sup> or SiC modified with 1% promoters ( $\text{ZrO}_2$ ,  $\text{CeO}_2$  and  $\text{Zr}_{0.5}\text{Ce}_{0.5}\text{O}_2$ ) and were prepared by the impregnation method. First,

0.4g SiC was added into 20ml aqueous solution of  $Zr(NO_3)_4 \cdot 5H_2O$  (0.05wt.%),  $Ce(NO_3)_3 \cdot 6H_2O$  (0.05wt.%) separately and into the above two nitrate mixture (Zr: 0.025wt.%; Ce: 0.025wt.%) under stirring for 12 hours. Afterwards all the mixtures were dried at 110°C for 12 hours and then calcined in air at 500°C for 4 hours. Then, 0.4g of SiC and the modified supports were separately added into 20ml  $Pd(NO_3)_2 \cdot 2H_2O$  aqueous solution (0.05wt.%); and we repeat the above method to prepare different 1wt.% Pd-based catalysts. The catalysts were marked as Pd/SiC, Pd/ $ZrO_2$ /SiC, Pd/ $CeO_2$ /SiC and Pd/ $Zr_{0.5}Ce_{0.5}O_2$ /SiC, respectively. For comparison, 1wt.% Pd/ $Al_2O_3$  catalyst was also prepared by impregnating  $\gamma-Al_2O_3$  ( $S_{BET}=160m^2/g$ ) with  $Pd(NO_3)_2 \cdot 2H_2O$  aqueous solution.

## 2.2 Catalytic test

The catalytic performance of the different catalysts for the methane combustion was carried out in a fixed-bed quartz reactor with an inner diameter of 8 mm at atmospheric pressure, and the mixture of  $O_2(20\%) / CH_4(1\%) / N_2(79\%)$  was used as the feedstock. 300 mg of the catalyst was packed between two layers of quartz wool. The hourly space velocity was controlled to be  $10000h^{-1}$ . Since the deactivation of the SiC-supported catalysts usually demands a long time, a repeated heating-then-cooling cycle method was employed to estimate the stabilities of the catalysts as previously reported<sup>[9]</sup>.

## 2.3 Catalyst characterization

The crystalline phases of different catalysts were characterized by a Rigaku D-Max/RB X-ray diffractometer (XRD) with Cu  $K\alpha$  radiation. The microstructures of the catalysts were analyzed by using a JEOL-2010 transmission electron microscope (TEM) and JEM-2010 high-resolution transmission electron microscope (HRTEM). X-ray photoelectron spectroscopy (XPS) were carried out on a Kratos XSAM800 spectrometer by using Al  $K\alpha$  ( $h\nu = 1486.6 eV$ ) X-ray source.

### 3. Results and discussion

#### 3.1 XRD and XPS characterization of fresh catalysts

From the XRD patterns of different fresh catalysts shown in Fig.1, the strong diffraction peak ( $2\theta=35.8^\circ$ ) can be indexed to  $\beta$ -SiC. All the catalysts present an obvious peak at  $2\theta=33.8^\circ$ , which attributed to the tetragonal PdO. Pd/ZrO<sub>2</sub>/SiC presents two peaks at near  $28.1^\circ$  and  $31.4^\circ$  ( $2\theta$ ), assigned to monoclinic ZrO<sub>2</sub>. The main peaks at  $28.8^\circ$  and  $33.3^\circ$  ( $2\theta$ ) in the XRD patterns of Pd/CeO<sub>2</sub>/SiC correspond to the cubic, fluorite structures of CeO<sub>2</sub>. The diffraction peaks ascribed to ZrO<sub>2</sub> were not observed in Pd/Zr<sub>0.5</sub>Ce<sub>0.5</sub>O<sub>2</sub>/SiC. However the  $2\theta$ -values of CeO<sub>2</sub> peaks increase from  $28.8^\circ$  and  $33.3^\circ$  to  $29.1^\circ$  and  $33.5^\circ$ , respectively. This is due to Zr<sup>4+</sup> has incorporated into the CeO<sub>2</sub> lattice, and caused the change of CeO<sub>2</sub> crystal phase and the formation of Zr<sub>0.5</sub>Ce<sub>0.5</sub>O<sub>2</sub> solid solution<sup>[20,21]</sup>.

Fig.2 represents the XPS spectra of fresh Pd/ZrO<sub>2</sub>/SiC, Pd/CeO<sub>2</sub>/SiC and Pd/Zr<sub>0.5</sub>Ce<sub>0.5</sub>O<sub>2</sub>/SiC. The peak at 337.6 - 337.7 eV shown in Fig.2a corresponds to the Pd 3d<sub>5/2</sub>. Generally, there are three components with Pd 3d<sub>5/2</sub> bonding energy (BE) values in 334.7-335.1 eV, 337.6-337.8 eV and 338.4-338.5 eV, which are usually attributed to Pd<sup>0</sup>, Pd<sup>2+</sup> and Pd<sup>4+</sup>, respectively<sup>[22-24]</sup>. Therefore, the valence of Pd atoms in these three catalysts is +2. The peaks of Pd/ZrO<sub>2</sub>/SiC at about 181.4 and 183.7 eV shown in Fig.2b correspond to the Zr 3d<sub>5/2</sub> and Zr 3d<sub>3/2</sub>, respectively. The difference in the binding energies between the Zr 3d<sub>5/2</sub> and Zr 3d<sub>3/2</sub> photoemission feature is 2.3 eV, which is in agreement with the reported value<sup>[25]</sup>. Nelson and Schulz reported that the band located at 900.2-900.6 eV was the Ce 3d<sub>3/2</sub> ionization and the band located at 881.7-882.0 eV was the Ce 3d<sub>5/2</sub> ionization<sup>[25]</sup>. Therefore, the peaks of Pd/CeO<sub>2</sub>/SiC at about 900.2 and 881.7eV shown in Fig. 2c should be the principal binding energies of Ce 3d<sub>3/2</sub> and Ce 3d<sub>5/2</sub>, respectively. The

peaks at about 897.6 and 916.1 eV are satellites arising from the Ce 3d<sub>3/2</sub> and Ce 3d<sub>5/2</sub>. According to the literature, in the Ce-Zr mixed oxide with 15-80% of Ce the peak position of Zr 3d<sub>5/2</sub> usually occurs at 181.7-181.8 eV and the Ce 3d<sub>5/2</sub> peak at 881.8-882.1 eV<sup>[26]</sup>. In the case of our study, the peak of Pd/Zr<sub>0.5</sub>Ce<sub>0.5</sub>O<sub>2</sub>/SiC at about 181.7 eV (Fig.2b) corresponds to the Zr 3d<sub>5/2</sub>, while the peak of Pd/Zr<sub>0.5</sub>Ce<sub>0.5</sub>O<sub>2</sub>/SiC at about 882.1 eV (Fig.2c) corresponds to the Ce 3d<sub>5/2</sub>. Thus, the majority of ZrO<sub>2</sub> and CeO<sub>2</sub> of Pd/Zr<sub>0.5</sub>Ce<sub>0.5</sub>O<sub>2</sub>/SiC are in the form of Ce<sub>0.5</sub>Zr<sub>0.5</sub>O<sub>2</sub> solid solution but not in the form of separate ZrO<sub>2</sub> and CeO<sub>2</sub>. From Fig.2c, the peak of Pd/Zr<sub>0.5</sub>Ce<sub>0.5</sub>O<sub>2</sub>/SiC at about 900.8 eV is the principal binding energies of Ce 3d<sub>3/2</sub>, and the peaks at about 897.8 eV and 916.3 eV are satellites arising from the Ce 3d<sub>3/2</sub> and Ce 3d<sub>5/2</sub>.

### 3.2 TEM and HRTEM characterization

Fig.3 shows TEM images of fresh and used Pd/SiC catalysts. From Fig.3a, the lattice spacings of nanoparticle are 0.262 nm and 0.269 nm, which are indexed as the (101) and (002) planes of tetragonal PdO. The PdO nanoparticles in Pd/SiC have a narrow size distribution from 2 to 4 nm and an average diameter of 2.6 nm according to our statistical analysis (Fig.3a). From Fig.3b, the lattice spacing of nanoparticles is 0.263 nm, which corresponds to (101) planes of tetragonal PdO, claiming the active phase PdO has not been decomposed into metallic Pd during the cyclic reaction. The average size of PdO particles only has a slight increase from 2.6 to 2.8 nm after the cyclic reaction (Fig.3b). The above results suggest that PdO nanoparticles are very stable on the surface of SiC because of the high thermal conductivity and chemical stability of the high surface area SiC, which can effectively hinder the sintering of active nanoparticles and thus stabilize them.

Fig.4 shows TEM images of fresh Pd/SiC catalysts modified by ZrO<sub>2</sub>, CeO<sub>2</sub> and Zr<sub>0.5</sub>Ce<sub>0.5</sub>O<sub>2</sub>. PdO nanoparticles could not be found in Fig.4 possibly because they are too small to be found out.

The lattice spacing of nanoparticles is 0.205 nm, which is attributed to the interplanar spacing of (211) plane of monoclinic  $\text{ZrO}_2$  (Fig.4a). The lattice spacings of 0.311, 0.312, 0.315 and 0.276 nm are indexed as the (111) and (200) of cubic  $\text{CeO}_2$  (Fig.4b). The lattice spacing of 0.291 nm corresponds to the (111) planes of cubic  $\text{Zr}_{0.5}\text{Ce}_{0.5}\text{O}_2$ . Compared with pure  $\text{CeO}_2$ , the interplanar spacing has a little decrease, suggesting that  $\text{Zr}^{4+}$  has inserted into the  $\text{CeO}_2$  crystal lattice, which may cause the change of  $\text{CeO}_2$  crystal phase<sup>[21]</sup>.

### 3.3 Catalytic performances

Fig.5 shows the results of activities and stabilities of different catalysts. From Fig.5a,  $T_{10\%}$  (temperature of 10% methane conversion) and  $T_{100\%}$  (temperature of methane complete conversion) of Pd/SiC is 285°C and 370°C respectively, which are nearly equal to those of Pd/ $\text{Al}_2\text{O}_3$  catalyst.  $\text{ZrO}_2$  modification can reduce  $T_{10\%}$  from 285°C to 230°C and  $T_{100\%}$  from 370°C to 350°C because  $\text{ZrO}_2$  excellent low temperature activity, oxygen storage capacity and transfer ability.  $\text{CeO}_2$  modification can reduce  $T_{10\%}$  from 285°C to 245°C and  $T_{100\%}$  from 370°C to 360°C, separately.  $\text{CeO}_2$  could increase the oxidizability of crystal boundary and form a synergistic effect between the active phases and supports, therefore improve the catalytic activity and stability<sup>[12,13]</sup>. Nevertheless,  $\text{Zr}_{0.5}\text{Ce}_{0.5}\text{O}_2$  solid solution modification can significantly reduce  $T_{10\%}$  from 285°C to 240°C and  $T_{100\%}$  from 370°C to 340°C respectively, suggesting that  $\text{Zr}_{0.5}\text{Ce}_{0.5}\text{O}_2$  solid solution could strongly improve oxygen storage capacity and thermal resistance<sup>[14-17]</sup>. This also means that the combustion reaction could be finished in a narrow temperature range (around 100°C).

Fig.5b shows the results of stability of Pd/ $\text{Al}_2\text{O}_3$ . The final methane conversion left only 67.4% at 370°C after 10 reaction cycles mainly because of the sintering of  $\gamma$ -alumina and coalescence of PdO nanoparticles<sup>[4, 5, 27]</sup>. However, the Pd/SiC (Fig.5c) and Pd/ $\text{Zr}_{0.5}\text{Ce}_{0.5}\text{O}_2$ /SiC (Fig.5d) catalysts

can keep the methane conversion at almost 100 % after 10 reaction cycles, indicating that high surface area SiC supported catalysts have excellent stability in methane combustion. This further confirms the previous results from TEM images of catalysts that high surface area SiC can significantly hinder the migration and coalescence of active phase nanoparticles and thus stabilize them.

#### **4. Conclusion**

Pd-based catalysts using high surface area SiC ( $50.8\text{m}^2/\text{g}$ ) modified by  $\text{CeO}_2$ ,  $\text{ZrO}_2$  and  $\text{Ce}_{0.5}\text{Zr}_{0.5}\text{O}_2$  solid solution as the support could effectively increase the dispersion and activity of active metallic phases. XRD and XPS studies showed that  $\text{Zr}^{4+}$  could be incorporated into the  $\text{CeO}_2$  lattice to form  $\text{Zr}_{0.5}\text{Ce}_{0.5}\text{O}_2$  solid solution.  $T_{10\%}$  and  $T_{100\%}$  of  $\text{Pd}/\text{Zr}_{0.5}\text{Ce}_{0.5}\text{O}_2/\text{SiC}$  are  $240^\circ\text{C}$  and  $340^\circ\text{C}$  respectively and the reaction could be finished in a narrow temperature range (around  $100^\circ\text{C}$ ) certainly due to the excellent oxygen storage capacity, redox properties, thermal stability and low temperature catalytic activity of  $\text{Ce}_{0.5}\text{Zr}_{0.5}\text{O}_2$  solid solution. However,  $\text{Pd}/\text{CeO}_2/\text{SiC}$  and  $\text{Pd}/\text{ZrO}_2/\text{SiC}$  have lower catalytic activity than  $\text{Pd}/\text{Zr}_{0.5}\text{Ce}_{0.5}\text{O}_2/\text{SiC}$ . All the SiC-based catalysts can keep the methane conversion of almost 100 % after 10 reaction cycles suggesting that active nanoparticles are well stabilized on the SiC surface while the promoters serve as oxygen reservoir and retain good redox properties.

#### **Acknowledgment**

The work was financially supported by Shanxi Province (Ref: 2008011014-1), NSFC (20973190) and MOST (Ref: SKLCC-2008BWZ010 and 2011CB201405).

#### **References**

[1] D. Ciuparu, M. R. Lyubovsky, E. Altman, L. D. Pfefferle, A. Datye, *Catal. Rev.* 44 (2002) 593.

- [2] P. Gélín, M. Primet, *Appl. Catal. B* 39 (2002) 1.
- [3] R. J. Farrauto, J. K. Lampert, M. C. Hobson, E. M. Waterman, *Appl. Catal. B* 6 (1995) 263.
- [4] F. X. Yin, S. F. Ji, P. Y. Wu, F. Z. Zhao, C. Y. Li, *J. Catal.* 257 (2008) 108.
- [5] Y. Ozawa, Y. Tochihara, A. Watanabe, M. Nagai, S. Omi, *Appl. Catal. A* 259 (2004) 1.
- [6] R. J. Shang, Y. Y. Wang, G. Q. Jin, X. Y. Guo, *Catal. Commun.* 10 (2009) 1502.
- [7] S. Ivanova, E. Vanhaecke, L. Dreibine, B. Louis, C. Pham, C. Pham-Huu, *Appl. Catal. A* 359 (2009) 151.
- [8] A. Berthet, A. L. Thomann, F. J. Cadete Santos Aires, M. Brun, C. Deranlot, J. C. Bertolini, J. P. Rozenbaum, P. Brault, P. Andreatza, *J. Catal.* 190 (2000) 49.
- [9] X. N. Guo, R. J. Shang, D. H. Wang, G. Q. Jin, X. Y. Guo, K. N. Tu, *Nanoscale Res. Lett.* 5 (2010) 332.
- [10] J. Krishna Murthy, S. Chandra Shekar, V. Siva Kumar, K. S. Rama Rao, *Catal. Commun.* 3 (2002) 145.
- [11] C. A. Müller, M. Maciejewski, R. A. Koepfel, A. Baiker, *Catal. Today* 47 (1999) 245.
- [12] S. Colussi, A. Trovarelli, G. Groppi, J. Llorca, *Catal. Commun.* 8 (2007) 1263.
- [13] P. O. Thevenin, A. Alcalde, L. J. Pettersson, S. G. Järås, J. L. G. Fierro, *J. Catal.* 215 (2003) 78.
- [14] R. Di Monte, P. Fornasiero, J. Kašpar, P. Rumori, G. Gubitosa, M. Graziani, *Appl. Catal. B* 24 (2000) 157.
- [15] M. Haneda, O. Houshito, T. Sato, H. Takagi, K. Shinoda, Y. Nakahara, K. Hiroe, H. Hamada, *Catal. Commun.* 11 (2010) 317.
- [16] P. Fornasiero, R. Di Monte, G. Rsga Rao, J. Kaspar, S. Meriani, A. Trovarelli, M. Graziani, J.

Catal. 151 (1995) 168.

[17] G. Balducci, P. Fornasiero, R. Di Monte, J. Kaspar, S. Meriani, M. Graziani, Catal. Lett. 33 (1995) 193.

[18] G. Q. Jin, X. Y. Guo, Micropor. Mesopor. Mat. 60 (2003) 207.

[19] X. Y. Guo, G. Q. Jin, J. Mater. Sci. 40 (2005) 1301.

[20] S. P. Wang, X. C. Zheng, X. Y. Wang, S. R. Wang, S. M. Zhang, L. H. Yu, W. P. Huang, S. H. Wu, Catal. Lett. 105 (2005) 163.

[21] G. Vlaic, R. Di Monte, P. Fornasiero, E. Fonda, J. Kašpar, M. Graziani, J. Catal. 182 (1999) 378.

[22] N. Ikeo, Y. Iijima, N. Nimura, M. Sigematsu, T. Tazawa, S. Matsumoto, K. Kojima, Y. Nagasawa, Handbook of X-Ray Photoelectron Spectroscopy, JEOL, Tokyo, 1991.

[23] L. M. T. Simplicio, S. T. Brandão, E. A. Sales, L. Lietti, F. Bozon-Verduraz, Appl. Catal. B 63 (2006) 9.

[24] K. Otto, L. P. Haack, J. E. deVries, Appl. Catal. B 1 (1992) 1.

[25] A. E. Nelson, K. H. Schulz, Appl. Surf. Sci. 210 (2003) 206.

[26] A. Galtayries, R. Sporken, J. Riga, G. Blanchard, R. Caudano, J. Electron Spectrosc. Rel. Phen. 88 (1998) 951.

[27] H. Arai, M. Machida, Catal. Today 10 (1991) 81.

### Figures captions:

Fig. 1 XRD patterns of different catalysts.

Fig. 2 XPS patterns of Pd/ZrO<sub>2</sub>/SiC, Pd/CeO<sub>2</sub>/SiC and Pd/Zr<sub>0.5</sub>Ce<sub>0.5</sub>O<sub>2</sub>/SiC: (a) Pd 3d, (b) Zr 3d and (c) Ce 3d.

Fig. 3 TEM images of fresh (a) and used (b) Pd/SiC, and the inserted figures are the HRTEM of different catalysts themselves.

Fig. 4 TEM images of different fresh modified catalysts: Pd/ZrO<sub>2</sub>/SiC (a), Pd/CeO<sub>2</sub>/SiC (b) and Pd/Zr<sub>0.5</sub>Ce<sub>0.5</sub>O<sub>2</sub>/SiC (c); and the inserted figures are HRTEM of different catalysts themselves.

Fig. 5 Catalytic performances of different catalysts for methane combustion: the activities of different catalysts (a); and cyclic reaction results of Pd/Al<sub>2</sub>O<sub>3</sub> (b), Pd/SiC (c) and Pd/Zr<sub>0.5</sub>Ce<sub>0.5</sub>O<sub>2</sub>/SiC (d).

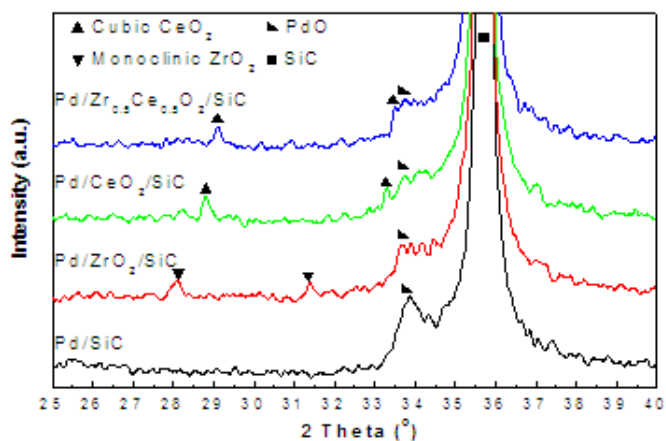


Fig. 1 XRD patterns of different catalysts.

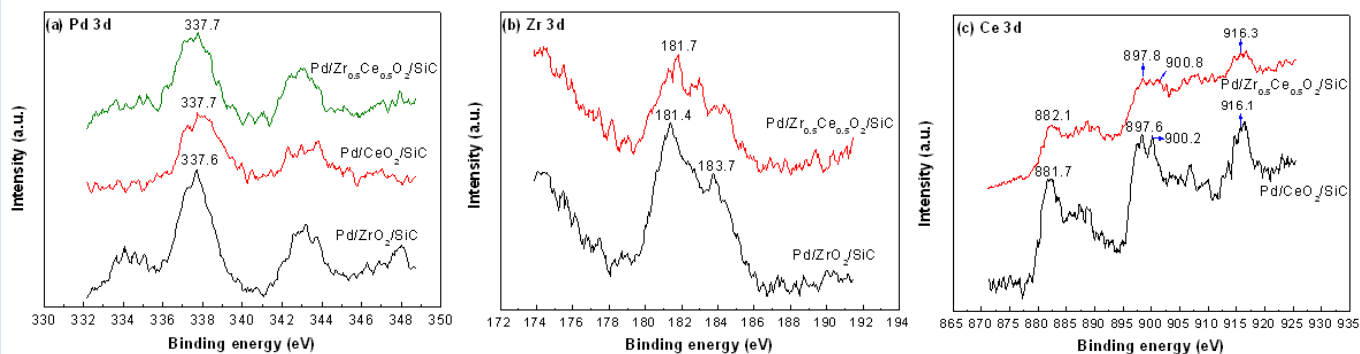


Fig. 2 XPS patterns of Pd/ZrO<sub>2</sub>/SiC, Pd/CeO<sub>2</sub>/SiC and Pd/Zr<sub>0.5</sub>Ce<sub>0.5</sub>O<sub>2</sub>/SiC: (a) Pd 3d, (b) Zr 3d and (c) Ce 3d.

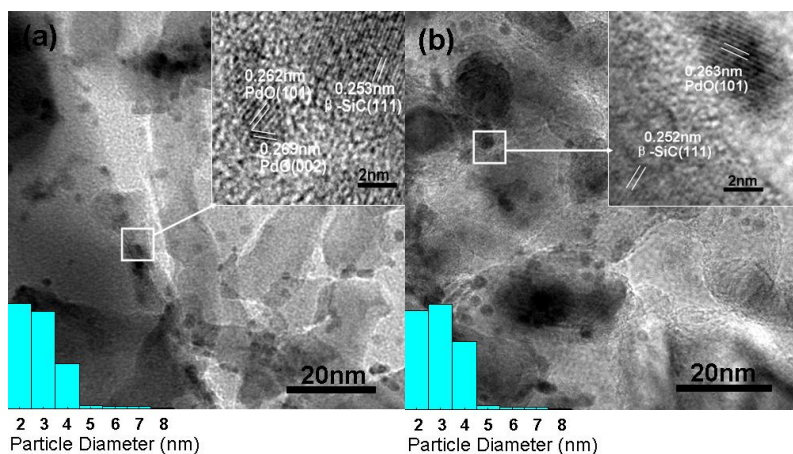


Fig. 3 TEM images of fresh (a) and used (b) Pd/SiC, and the inserted figures are the HRTEM of different catalysts themselves.

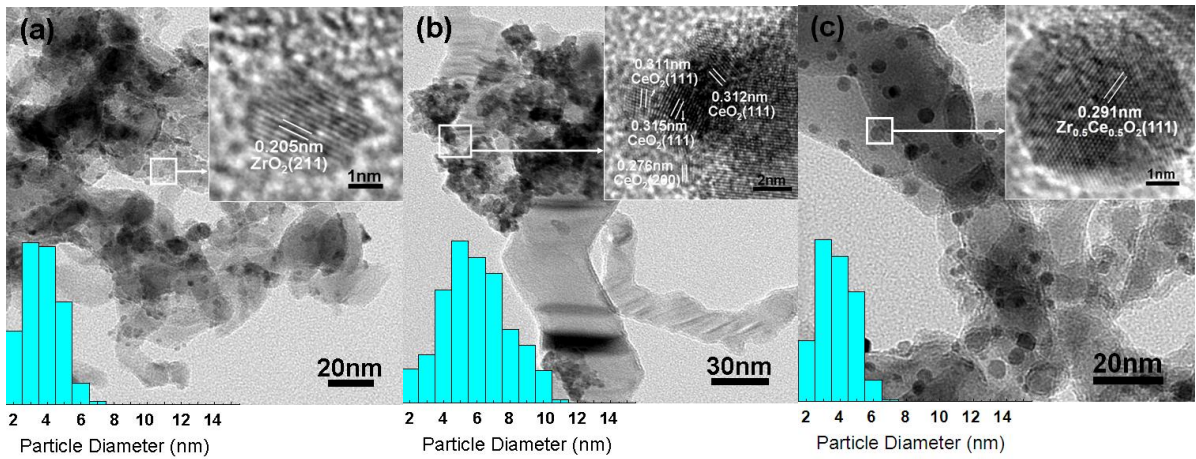


Fig. 4 TEM images of different fresh modified catalysts: Pd/ZrO<sub>2</sub>/SiC (a), Pd/CeO<sub>2</sub>/SiC (b) and Pd/Zr<sub>0.5</sub>Ce<sub>0.5</sub>O<sub>2</sub>/SiC (c); and the inserted figures are HRTEM of different catalysts themselves.

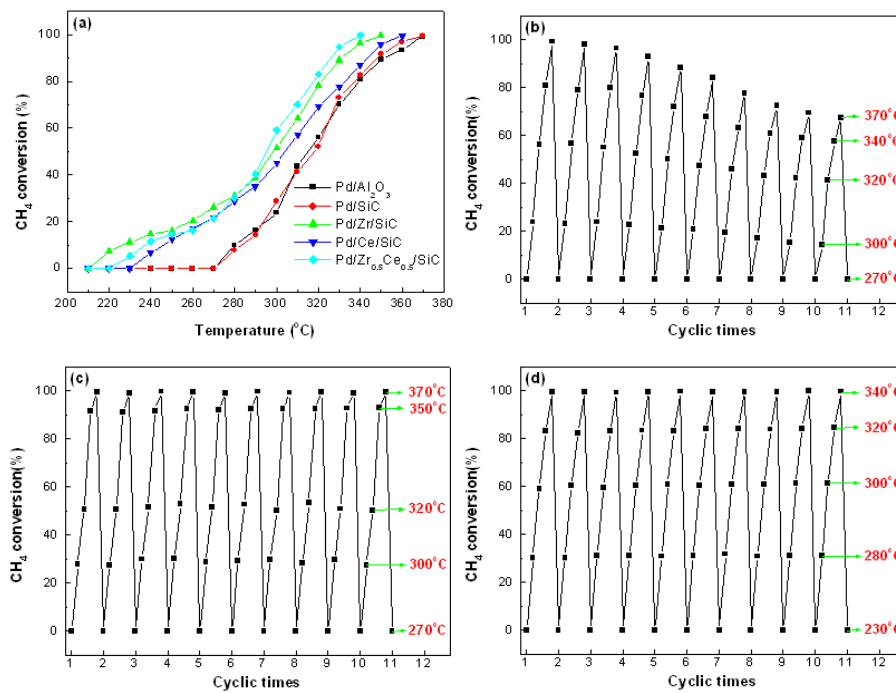


Fig. 5 Catalytic performances of different catalysts for methane combustion: the activities of different catalysts (a); and cyclic reaction results of Pd/Al<sub>2</sub>O<sub>3</sub> (b), Pd/SiC (c) and Pd/Zr<sub>0.5</sub>Ce<sub>0.5</sub>O<sub>2</sub>/SiC (d).